# High-Order Curvilinear Finite Elements for Lagrangian Hydrodynamics

## Part I: General Framework

Veselin Dobrev, Tzanio Kolev and Robert Rieben

Lawrence Livermore National Laboratory

Numerical Methods for Multi-Material Fluid Flows

Arcachon, France, Sept. 5th–9th, 2011

LLNL-PRES-497394

This work performed under the auspices of the U.S. Department of Energy by Lawrence Livermore National Laboratory under Contract DE-AC52-07NA27344

# Euler's Equations in a Lagrangian Frame

The evolution of the particles of a compressible fluid/solid in a Lagrangian reference frame is governed by the following system of differential equations:

**Euler's Equations**

**Momentum Conservation:** $$\rho \frac{\mathrm{d}\vec{v}}{\mathrm{d}t} = \nabla \cdot \sigma$$

**Mass Conservation:** $$\frac{1}{\rho}\frac{\mathrm{d}\rho}{\mathrm{d}t} = -\nabla \cdot \vec{v}$$

**Energy Conservation:** $$\rho \frac{\mathrm{d}e}{\mathrm{d}t} = \sigma : \nabla \vec{v}$$

**Equation of State:** $$p = EOS(e, \rho)$$

**Equation of Motion:** $$\frac{\mathrm{d}\vec{x}}{\mathrm{d}t} = \vec{v}$$

**Kinematics**

| | | |
|---|---|---|
| $\vec{x}$ | – | position |
| $\vec{v}$ | – | velocity |

**Thermodynamics**

| | | |
|---|---|---|
| $\rho$ | – | density |
| $e$ | – | internal energy |

**Stress Tensor**

$$\sigma = -p\mathbf{I} + \mu\varepsilon(\vec{v}) + s$$

| | | |
|---|---|---|
| $p$ | – | pressure |
| $\mu$ | – | artificial viscosity coef. |
| $s$ | – | stress deviator tensor |

- Time derivatives are along particle trajectories
- Space derivatives are with respect to a fixed coordinate system
- Domain: $\Omega(t) = \{\vec{x}(t)\}$; Total Energy: $E(t) = \int_{\Omega(t)} (\rho|\vec{v}|^2/2 + \rho e)$

# Overview of Lagrangian Methods

## Staggered-grid hydro (SGH) methods

- M. Wilkins, Methods in Computational Physics, *Calculation of Elastic-Plastic Flow*, Academic Press, 1964
- E. Caramana and M. Shashkov, *Elimination of Artificial Grid Distortion and Hourglass-Type Motions by Means of Lagrangian Subzonal Masses and Pressures*, J. Comput. Phys., 142 (2), pp. 521–561, 1998
- E. Caramana, D. Burton, M. Shashkov and P. Whalen, *The Construction of Compatible Hydrodynamics Algorithms Utilizing Conservation of Total Energy*, J. Comput. Phys., 146, pp. 227–262, 1998

## Finite element based methods

- G. Scovazzi, M. Christon, T. Hughes and J. Shadid, *Stabilized shock hydrodynamics: I. A Lagrangian method*, Comput. Methods Appl. Mech. Engrg., 196 (4-6), pp. 923–966, 2007.
- A. Barlow, *A compatible finite element multi-material ALE hydrodynamics algorithm*, Int. J. Numer. Meth. Fluids, 56, pp. 953–964, 2008.
- G. Scovazzi, E. Love and M. Shashkov, *Multi-Scale Lagrangian Shock Hydrodynamics on Q1/P0 finite elements: Theoretical framework and two-dimensional computations*, Comput. Methods Appl. Mech. Engrg., 197, pp. 1056–1079, 2008

## Cell-centered methods

- B. Depres and C. Mazeran, *Lagrangian Gas Dynamics in Two Dimensions and Lagrangian systems*, Arch. Rational Mech. Anal. 178 (2005), pp. 1781–1824, 2005.
- P.-H. Maire, R. Abgrall, J. Breil and J. Ovadia, *A cell-centered Lagrangian scheme for compressible flow problems*, SIAM J. Sci. Comput., 29 (4), pp. 1781–1824, 2007.
- P.-H. Maire, *A high-order cell-centered Lagrangian scheme for two-dimensional compressible fluid flows on unstructured meshes*, J. Comput. Phys., 228 (7), pp. 2391–2425, 2009.

# Lagrangian Mesh Motion

- Semi-discrete Lagrangian methods are based on a moving computational mesh

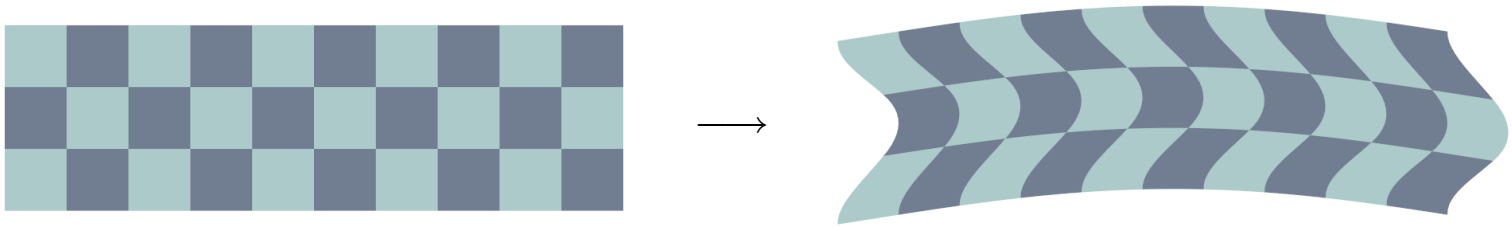

- The mesh zones are reconstructed based on particle locations, thus defining the moved mesh

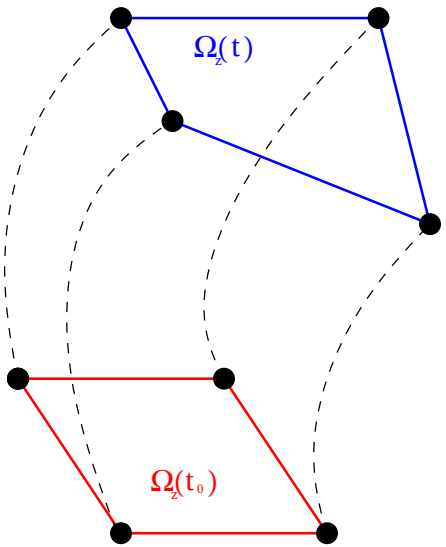


**$Q_1$ bilinear approximation**
(SGH)

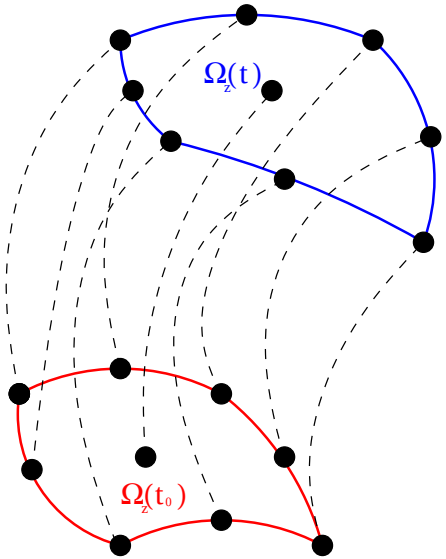


**$Q_2$ biquadratic approximation**
(FEM)

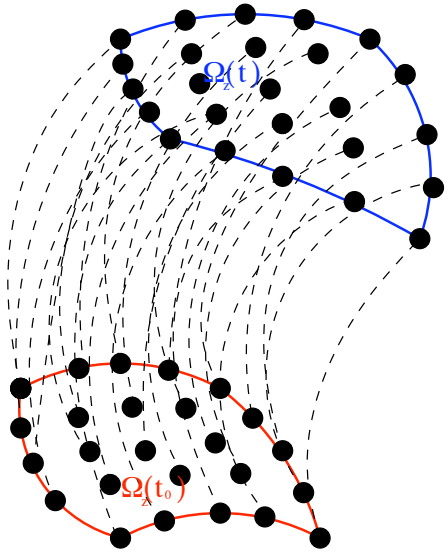


**$Q_4$ biquartic approximation**
(FEM)

- The reconstruction has an inherent geometric error with respect to the equation of motion

# Why Curvilinear Elements?

- Deform an initial Cartesian mesh with the exact solution

## Exact motion: Sedov blast wave

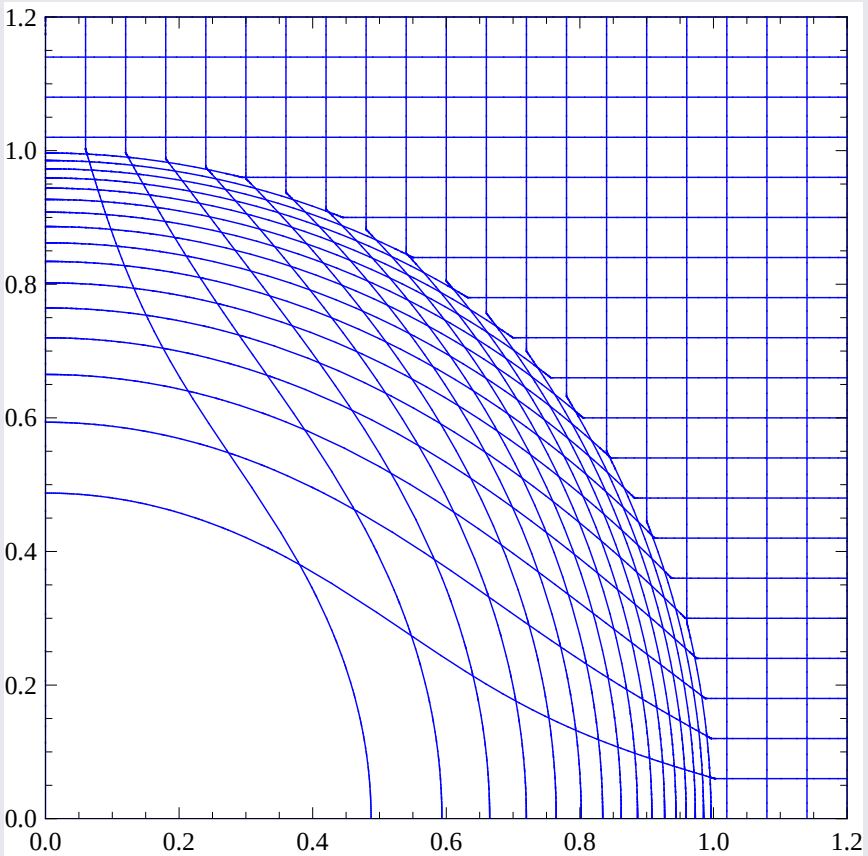


## Exact motion: Taylor–Green vortex

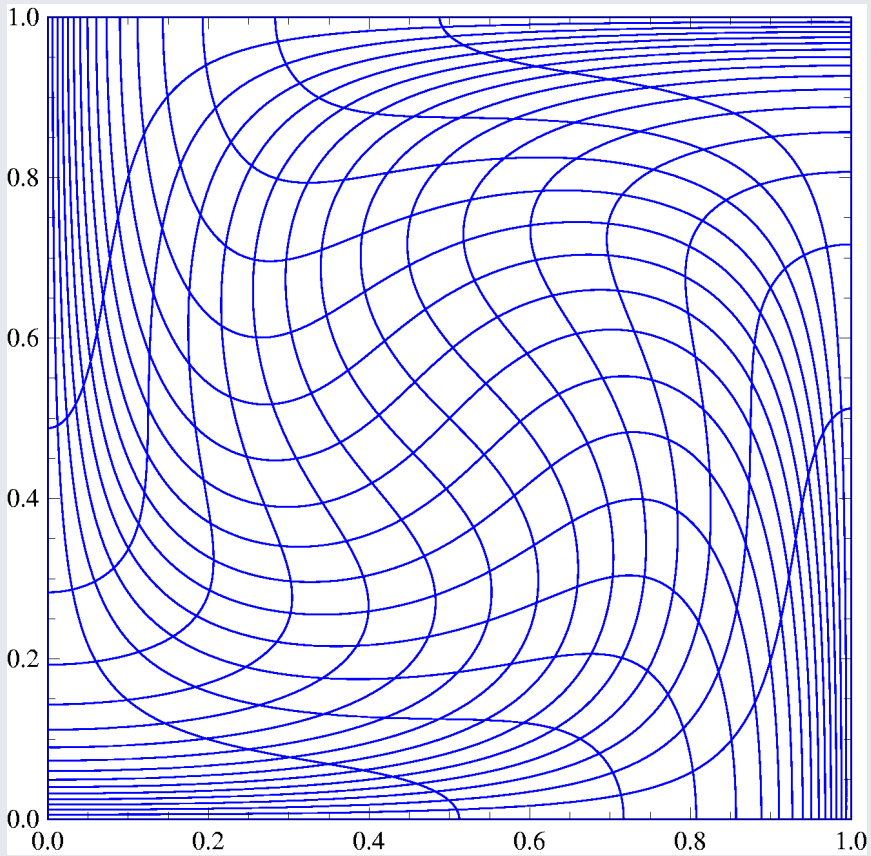


**High order curvilinear finite elements use additional particle degrees of freedom to more accurately represent the initial and the naturally developed curvature in the problem**

# Position

- Finite element zones are defined by a parametric mapping $\Phi_z$ from a reference zone (the unit square in 2D): $\Omega_z(t) = \{\vec{x} = \Phi_z(\hat{\vec{x}}, t) \ : \ \hat{\vec{x}} \in \hat{\Omega}_z\}$.

Reference Space ($\hat{\Omega}_z$)

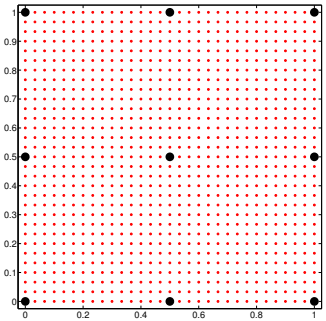

$\Phi_z$ $\longrightarrow$

Physical Space ($\Omega_z$)

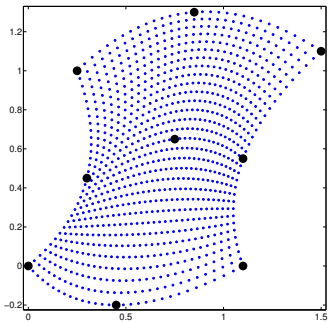

- The position space is specified by a set of nodal FEM basis functions $\{\hat{\eta}_i\}$ on $\hat{\Omega}_z$.

$\hat{\eta}_i \in Q_1$

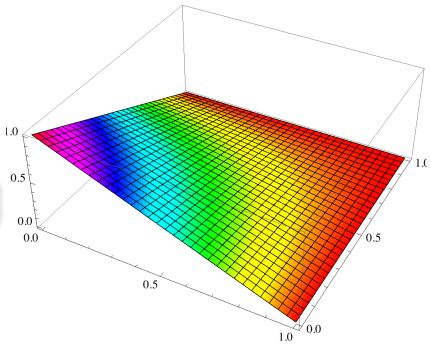

$\hat{\eta}_i \in Q_2$

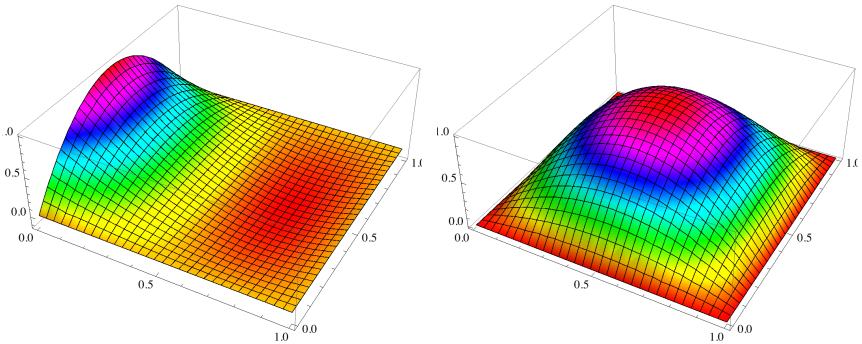

- The parametric mapping is then given by $\Phi_z(\hat{\vec{x}}, t) = \sum_i \mathbf{x}_{z,i}(t)\, \hat{\eta}_i(\hat{\vec{x}})$

The position vector $\mathbf{x}(t)$ specifies the particle coordinates corresponding to the degrees of freedom in the $\{\hat{\eta}_i\}$-defined finite element space

# Strong Mass Conservation

- For a bijective mapping, the Jacobian matrix

$$\mathbf{J}_z = \nabla_{\hat{\vec{x}}} \Phi_z \qquad \text{or} \qquad (\mathbf{J}_z)_{ij} = \frac{\partial x_j}{\partial \hat{x}_i}$$

  is non-singular. In general, $\mathbf{J}_z$ is a *function that varies inside the zone*.
- Determinant $|\mathbf{J}_z(t)|$ can be viewed as *local volume* since $V_z(t) = \int_{\hat{\Omega}_z} |\mathbf{J}_z(t)|$.

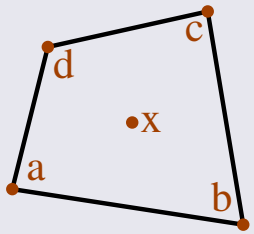


$|\mathbf{J}_z(a)| = 2S_{abd}$
$|\mathbf{J}_z(x)| = S_{abcd}$

# Strong Mass Conservation

- For a bijective mapping, the Jacobian matrix

$$\mathbf{J}_z = \nabla_{\hat{\vec{x}}} \Phi_z \qquad \text{or} \qquad (\mathbf{J}_z)_{ij} = \frac{\partial x_j}{\partial \hat{x}_i}$$

  is non-singular. In general, $\mathbf{J}_z$ is a *function that varies inside the zone*.

- Determinant $|\mathbf{J}_z(t)|$ can be viewed as *local volume* since $V_z(t) = \int_{\hat{\Omega}_z} |\mathbf{J}_z(t)|$.

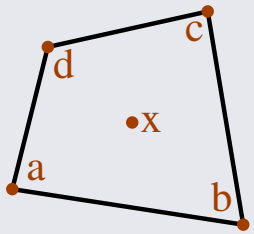


$|\mathbf{J}_z(a)| = 2S_{abd}$
$|\mathbf{J}_z(x)| = S_{abcd}$

- In the Lagrangian description, the total mass of a zone is constant for all time:

$$\frac{\mathrm{d}m_z}{\mathrm{d}t} = 0, \quad m_z = \int_{\Omega_z(t)} \rho$$

- The **strong mass conservation principle** takes this to the extreme by requiring that

$$\int_{\Omega'(t)} \rho(t) = \int_{\Omega'(t_0)} \rho(t_0) \quad \longrightarrow \quad \int_{\hat{\Omega}'} \hat{\rho}(t)|\mathbf{J}(t)| = \int_{\hat{\Omega}'} \hat{\rho}(t_0)|\mathbf{J}(t_0)|$$

for any $\Omega'(t_0) \subset \Omega(t_0)$. This leads to the pointwise equality $\rho(t)|\mathbf{J}_z(t)| = \rho(t_0)|\mathbf{J}_z(t_0)|$

# Strong Mass Conservation

- For a bijective mapping, the Jacobian matrix

$$\mathbf{J}_z = \nabla_{\hat{\vec{x}}} \Phi_z \qquad \text{or} \qquad (\mathbf{J}_z)_{ij} = \frac{\partial x_j}{\partial \hat{x}_i}$$

  is non-singular. In general, $\mathbf{J}_z$ is a *function that varies inside the zone.*

- Determinant $|\mathbf{J}_z(t)|$ can be viewed as *local volume* since $V_z(t) = \int_{\hat{\Omega}_z} |\mathbf{J}_z(t)|$.

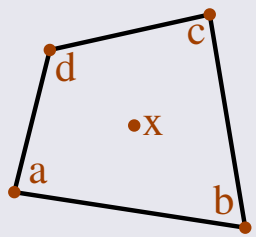


$|\mathbf{J}_z(a)| = 2S_{abd}$
$|\mathbf{J}_z(x)| = S_{abcd}$

- In the Lagrangian description, the total mass of a zone is constant for all time:

$$\frac{\mathrm{d}m_z}{\mathrm{d}t} = 0, \quad m_z = \int_{\Omega_z(t)} \rho$$

- The **strong mass conservation principle** takes this to the extreme by requiring that

$$\int_{\Omega'(t)} \rho(t) = \int_{\Omega'(t_0)} \rho(t_0) \quad \longrightarrow \quad \int_{\hat{\Omega}'} \hat{\rho}(t)|\mathbf{J}(t)| = \int_{\hat{\Omega}'} \hat{\rho}(t_0)|\mathbf{J}(t_0)|$$

  for any $\Omega'(t_0) \subset \Omega(t_0)$. This leads to the pointwise equality $\rho(t)|\mathbf{J}_z(t)| = \rho(t_0)|\mathbf{J}_z(t_0)|$

- Generalization of SGH zonal mass conservation
- $\hat{\rho}(t)$ is a non-polynomial *function* closely related to $|\mathbf{J}(t)|$
- **Density can be eliminated from the semi-discrete equations!**

# Kinematics

- Velocity is discretized in the same space as the position:

$$\vec{v}(\vec{x},t) \approx \sum_j \mathbf{v}_j(t)\,\vec{w}_j$$

- The velocity basis functions satisfy

$$\hat{\vec{w}}_j = \vec{w}_j \circ \Phi_z \in span\{\hat{\eta}_i\}^{dim}$$

- Let $\mathbf{w}(\vec{x},t)$ be a column vector of the velocity basis functions, i.e. $\mathbf{w}_j(\vec{x},t) = \vec{w}_j(\vec{x},t)$. Then

$$\vec{v}(\vec{x},t) \approx \mathbf{w}^{\mathsf{T}}\mathbf{v}$$

- Therefore, **the semi-discrete equation of motion** reads simply:

$$\frac{\mathrm{d}\mathbf{x}}{\mathrm{d}t} = \mathbf{v}$$

- Since $\hat{\vec{w}}_j$ is independent of time, $\vec{w}_j$ moves with the mesh and

$$\frac{\mathrm{d}\mathbf{w}}{\mathrm{d}t} = 0$$

**$Q_2$ kinematic degrees of freedom on the reference element**

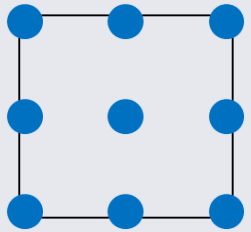

**$Q_2$ finite element basis function in physical space with degrees of freedom**

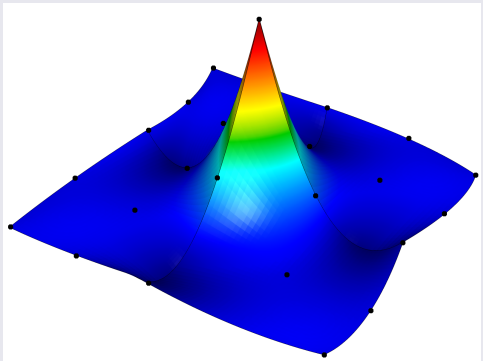

# Conservation of Momentum

Weak formulation of the momentum conservation equation:

$$\rho \frac{\mathrm{d}\vec{v}}{\mathrm{d}t} = \nabla \cdot \sigma \quad \longrightarrow \quad \int_{\Omega(t)} \rho \frac{\mathrm{d}\vec{v}}{\mathrm{d}t} \cdot \vec{w}_j = - \int_{\Omega(t)} \sigma : \nabla \vec{w}_j \, .$$

(the boundary integral is usually zero due to boundary conditions)

Since the velocity basis functions move with the mesh, we have

$$\frac{\mathrm{d}\vec{v}}{\mathrm{d}t} \approx \frac{\mathrm{d}}{\mathrm{d}t}(\mathbf{w}^\mathbf{T}\mathbf{v}) = \mathbf{w}^\mathbf{T} \frac{\mathrm{d}\mathbf{v}}{\mathrm{d}t}$$

# Conservation of Momentum

Weak formulation of the momentum conservation equation:

$$\rho \frac{\mathrm{d}\vec{v}}{\mathrm{d}t} = \nabla \cdot \sigma \quad \longrightarrow \quad \int_{\Omega(t)} \rho \frac{\mathrm{d}\vec{v}}{\mathrm{d}t} \cdot \vec{w}_j = -\int_{\Omega(t)} \sigma : \nabla \vec{w}_j \, .$$

(the boundary integral is usually zero due to boundary conditions)

Since the velocity basis functions move with the mesh, we have

$$\frac{\mathrm{d}\vec{v}}{\mathrm{d}t} \approx \frac{\mathrm{d}}{\mathrm{d}t}(\mathbf{w}^T \mathbf{v}) = \mathbf{w}^T \frac{\mathrm{d}\mathbf{v}}{\mathrm{d}t}$$

This gives us the **semi-discrete momentum conservation equation**:

$$\mathbf{M_v} \frac{\mathrm{d}\mathbf{v}}{\mathrm{d}t} = -\int_{\Omega} \sigma : \nabla \mathbf{w}$$

where the **velocity mass matrix** is defined by the integral

$$\mathbf{M_v} = \int_{\Omega} \rho \mathbf{w} \mathbf{w}^T$$

# Conservation of Momentum

Weak formulation of the momentum conservation equation:

$$\rho \frac{\mathrm{d}\vec{v}}{\mathrm{d}t} = \nabla \cdot \sigma \quad \longrightarrow \quad \int_{\Omega(t)} \rho \frac{\mathrm{d}\vec{v}}{\mathrm{d}t} \cdot \vec{w}_j = -\int_{\Omega(t)} \sigma : \nabla \vec{w}_j \,.$$

(the boundary integral is usually zero due to boundary conditions)

Since the velocity basis functions move with the mesh, we have

$$\frac{\mathrm{d}\vec{v}}{\mathrm{d}t} \approx \frac{\mathrm{d}}{\mathrm{d}t}(\mathbf{w}^T \mathbf{v}) = \mathbf{w}^T \frac{\mathrm{d}\mathbf{v}}{\mathrm{d}t}$$

This gives us the **semi-discrete momentum conservation equation**:

$$\mathbf{M_v} \frac{\mathrm{d}\mathbf{v}}{\mathrm{d}t} = -\int_{\Omega} \sigma : \nabla \mathbf{w}$$

where the **velocity mass matrix** is defined by the integral

$$\mathbf{M_v} = \int_{\Omega} \rho \mathbf{w} \mathbf{w}^T$$

By strong mass conservation, **the mass matrix is constant in time!**

$$\mathbf{M_v}(t)_{ij} = \int_{\Omega(t)} \rho \vec{w}_i \cdot \vec{w}_j = \int_{\hat{\Omega}(t)} \hat{\rho} |\mathbf{J}(t)| \hat{\vec{w}}_i \cdot \hat{\vec{w}}_j = \mathbf{M_v}(t_0)_{ij} \qquad \text{so} \qquad \boxed{\frac{\mathrm{d}\mathbf{M_v}}{\mathrm{d}t} = \mathbf{0}}$$

# Connection to Classical SGH

## Connection to Nodal Mass

The velocity mass matrix is computed by assembling individual zonal mass matrices

$$\mathbf{M_v} = Assemble(\mathbf{M}_z).$$

Each zonal mass matrix is block diagonal

$$\mathbf{M}_z = \int_{\Omega_z} \rho \mathbf{w}\mathbf{w}^T = \begin{pmatrix} \mathbf{M}_z^{xx} & 0 \\ 0 & \mathbf{M}_z^{yy} \end{pmatrix}.$$

Using a bilinear velocity basis and applying single point quadrature and mass lumping to the zonal mass matrix yields

$$\mathbf{M}_z^{xx} = \mathbf{M}_z^{yy} = \frac{\rho_z V_z}{16} \begin{pmatrix} 4 & 0 & 0 & 0 \\ 0 & 4 & 0 & 0 \\ 0 & 0 & 4 & 0 \\ 0 & 0 & 0 & 4 \end{pmatrix}.$$

This is equivalent to defining nodal masses as $\frac{1}{4}$ the mass of the surrounding zonal masses.

## Connection to SGH Gradient Operator

Consider the case of piecewise constant stresses, bilinear velocities and single point quadrature

$$\int_{\Omega_z} p\mathbf{I} : \nabla \mathbf{w} =$$

$$\frac{p_z}{2} \begin{pmatrix} y_2 - y_4, y_3 - y_1, y_4 - y_2, y_1 - y_3 \\ x_4 - x_2, x_1 - x_3, x_2 - x_4, x_3 - x_1 \end{pmatrix}.$$

The resulting "corner forces" are identical to the Wilkins and compatible hydro gradient operators on general quad grids.

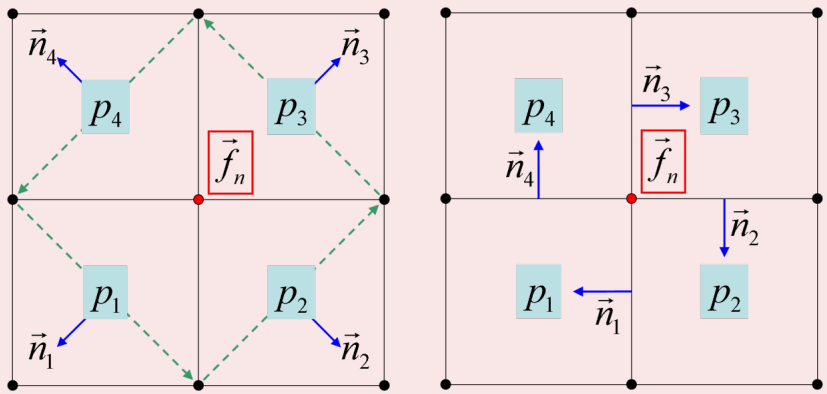

# Thermodynamics

Internal energy is approximated with a set of discontinuous basis functions $\phi$:

$$e(\vec{x}, t) \approx \boldsymbol{\phi}^{\mathsf{T}} \mathbf{e}$$

Weak formulation of the energy conservation equation for each zone

$$\int_{\Omega_z(t)} \left( \rho \frac{\mathrm{d}e}{\mathrm{d}t} \right) \phi_j = \int_{\Omega_z(t)} (\sigma : \nabla \vec{v})\, \phi_j$$

Since the basis functions move with the mesh, we have

$$\frac{\mathrm{d}\boldsymbol{\phi}}{\mathrm{d}t} = \mathbf{0} \quad \longrightarrow \quad \frac{\mathrm{d}e}{\mathrm{d}t} \approx \boldsymbol{\phi}^{\mathsf{T}} \frac{\mathrm{d}\mathbf{e}}{\mathrm{d}t}$$

This gives us the **semi-discrete energy conservation equation**:

$$\mathbf{M}_e \frac{\mathrm{d}\mathbf{e}}{\mathrm{d}t} = \int_{\Omega} (\sigma : \nabla \vec{v})\, \boldsymbol{\phi}$$

where the **constant energy mass matrix** is defined by the integral

$$\mathbf{M}_e = \int_{\Omega} \rho \boldsymbol{\phi} \boldsymbol{\phi}^{\mathsf{T}}$$

**$Q_1$ thermodynamics degrees of freedom on the reference element**

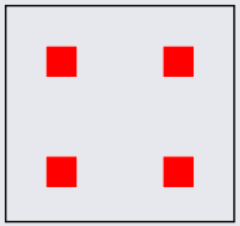

**Discontinuous $Q_1$ finite element function with degrees of freedom**

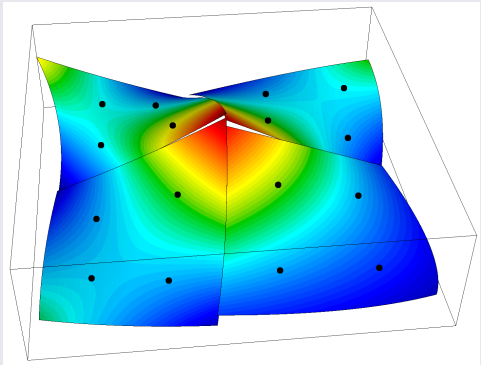

Since the FEM space is discontinuous, $\mathbf{M}_e$ is *block-diagonal* and the above equation reduces to separate equations local to each zone.

# Connection to Classical SGH

Consider the special case of piece wise constant internal energies, pressures and densities. For each zone, our general high order semi-discrete energy conservation law reduces to the form

$$\mathbf{M_e}\frac{\mathrm{d}\mathbf{e}}{\mathrm{d}t} = \int_\Omega (\sigma : \nabla\vec{v})\,\phi \quad \mapsto \quad m_z\frac{\mathrm{d}e_z}{\mathrm{d}t} = \mathbf{f}_z \cdot \mathbf{v}_z$$

## Connection to Compatible Hydro

Our method can be viewed as a high order generalization of the energy conserving compatible formulation [1] by noting that

$$\mathbf{f}_z = \int_{\Omega_z} p\mathbf{I} : \nabla\mathbf{w},$$

which is a collection of corner forces. The total change in energy is therefore given by the inner product

$$\mathbf{f}_z \cdot \mathbf{v}_z = \sum_{j=1}^{4} \vec{f}_j \cdot \vec{v}_j$$

[1] E. Caramana et. al., "The Construction of Compatible Hydrodynamics Algorithms Utilizing Conservation of Total Energy", J. Comput. Phys., 1998

## Connection to Wilkins Hydro

Assuming piecewise constant stresses, the right hand side is

$$\mathbf{f}_z \cdot \mathbf{v}_z = p_z\left(\int_{\Omega_z} \mathbf{I} : \nabla\mathbf{w}\right)\cdot\mathbf{v}_z \approx p_z\int_{\Omega_z}\nabla\cdot\vec{v}.$$

Using the geometric conservation law, this last term is equivalent to

$$p_z\int_{\Omega_z}\nabla\cdot\vec{v} = p_z\frac{\mathrm{d}V_z}{\mathrm{d}t}.$$

This is the so called "pdV" approach which has the potential to preserve entropy for adiabatic flows.

# Stress: Tensor Artificial Viscosity

We introduce artificial viscosity by adding an artificial stress tensor $\sigma_a$ to the stress tensor $\sigma$:

$$\sigma(\vec{x}) = -p(\vec{x})\mathbf{I} + \sigma_a(\vec{x}).$$

Note that, in general, both the pressure and the artificial stress vary inside a zone.

# Stress: Tensor Artificial Viscosity

We introduce artificial viscosity by adding an artificial stress tensor $\sigma_a$ to the stress tensor $\sigma$:

$$\sigma(\vec{x}) = -p(\vec{x})\mathbf{I} + \sigma_a(\vec{x}).$$

Note that, in general, both the pressure and the artificial stress vary inside a zone.

We have implemented the following options:

$\sigma_a = \mu_{\vec{s}} \nabla \vec{v}$ $\quad$ $\sigma_a = \mu_{\vec{s}}\, \varepsilon(\vec{v})$ $\quad$ $\sigma_a = \mu_{\vec{s}_k} \lambda_k \vec{s}_k \otimes \vec{s}_k$ $\quad$ $\sigma_a = \sum_k \mu_{\vec{s}_k} \lambda_k \vec{s}_k \otimes \vec{s}_k$

$\varepsilon(\vec{v})$ is the symmetrized velocity gradient with eigenvalues $\{\lambda_k\}$ and eigenvectors $\{\vec{s}_k\}$, i.e.

$$\varepsilon(\vec{v}) = \frac{1}{2}(\nabla \vec{v} + \vec{v}\nabla) = \sum_k \lambda_k \vec{s}_k \otimes \vec{s}_k, \qquad \vec{s}_i \cdot \vec{s}_j = \delta_{ij}, \qquad \lambda_1 \leq \cdots \leq \lambda_d$$

All $\sigma_a$ are symmetric, except $\mu_{\vec{s}} \nabla \vec{v}$ when $\nabla \times \vec{v} \neq \vec{0}$, and satisfy $\sigma_a(\vec{x}) : \nabla \vec{v}(\vec{x}) \geq 0$, $\forall \vec{x}$.

# Stress: Tensor Artificial Viscosity

We introduce artificial viscosity by adding an artificial stress tensor $\sigma_a$ to the stress tensor $\sigma$:

$$\sigma(\vec{x}) = -p(\vec{x})\mathbf{I} + \sigma_a(\vec{x}).$$

Note that, in general, both the pressure and the artificial stress vary inside a zone.

We have implemented the following options:

$\sigma_a = \mu_{\vec{s}} \nabla \vec{v}$ $\quad$ $\sigma_a = \mu_{\vec{s}}\, \varepsilon(\vec{v})$ $\quad$ $\sigma_a = \mu_{\vec{s}_k} \lambda_k \vec{s}_k \otimes \vec{s}_k$ $\quad$ $\sigma_a = \sum_k \mu_{\vec{s}_k} \lambda_k \vec{s}_k \otimes \vec{s}_k$

$\varepsilon(\vec{v})$ is the symmetrized velocity gradient with eigenvalues $\{\lambda_k\}$ and eigenvectors $\{\vec{s}_k\}$, i.e.

$$\varepsilon(\vec{v}) = \frac{1}{2}(\nabla \vec{v} + \vec{v}\nabla) = \sum_k \lambda_k \vec{s}_k \otimes \vec{s}_k, \qquad \vec{s}_i \cdot \vec{s}_j = \delta_{ij}, \qquad \lambda_1 \leq \cdots \leq \lambda_d$$

Directional viscosity coefficient:

$$\mu_{\vec{s}} = \mu_{\vec{s}}(\vec{x}) \equiv \rho \left\{ q_2 \ell_{\vec{s}}^2 |\Delta_{\vec{s}} \vec{v}| + q_1 \psi_0 \psi_1 \ell_{\vec{s}} c_s \right\}$$

$q_1$, $q_2$ – linear/quadratic term scaling; $c_s$ – speed of sound; $\ell_{\vec{s}} = \ell_{\vec{s}}(\vec{x})$ – directional length scale

# Stress: Tensor Artificial Viscosity

We introduce artificial viscosity by adding an artificial stress tensor $\sigma_a$ to the stress tensor $\sigma$:

$$\sigma(\vec{x}) = -p(\vec{x})\mathbf{I} + \sigma_a(\vec{x}).$$

Note that, in general, both the pressure and the artificial stress vary inside a zone.

We have implemented the following options:

$\sigma_a = \mu_{\vec{s}} \nabla \vec{v}$ $\quad$ $\sigma_a = \mu_{\vec{s}}\, \varepsilon(\vec{v})$ $\quad$ $\sigma_a = \mu_{\vec{s}_k} \lambda_k \vec{s}_k \otimes \vec{s}_k$ $\quad$ $\sigma_a = \sum_k \mu_{\vec{s}_k} \lambda_k \vec{s}_k \otimes \vec{s}_k$

$\varepsilon(\vec{v})$ is the symmetrized velocity gradient with eigenvalues $\{\lambda_k\}$ and eigenvectors $\{\vec{s}_k\}$, i.e.

$$\varepsilon(\vec{v}) = \frac{1}{2}(\nabla \vec{v} + \vec{v}\nabla) = \sum_k \lambda_k \vec{s}_k \otimes \vec{s}_k, \qquad \vec{s}_i \cdot \vec{s}_j = \delta_{ij}, \qquad \lambda_1 \leq \cdots \leq \lambda_d$$

Directional viscosity coefficient:

$$\mu_{\vec{s}} = \mu_{\vec{s}}(\vec{x}) \equiv \rho \left\{ q_2 \ell_{\vec{s}}^2 |\Delta_{\vec{s}} \vec{v}| + q_1 \psi_0 \psi_1 \ell_{\vec{s}} c_s \right\}$$

$q_1$, $q_2$ – linear/quadratic term scaling; $c_s$ – speed of sound; $\ell_{\vec{s}} = \ell_{\vec{s}}(\vec{x})$ – directional length scale

Directional measure of compression:

$$\Delta_{\vec{s}} \vec{v} = \frac{\vec{s} \cdot \nabla \vec{v} \cdot \vec{s}}{\vec{s} \cdot \vec{s}} = \frac{\vec{s} \cdot \varepsilon(\vec{v}) \cdot \vec{s}}{\vec{s} \cdot \vec{s}} \left[ = \frac{\mathrm{d}(\vec{v} \cdot \vec{s})}{\mathrm{d}\vec{s}} \right]$$

Compression switch, vorticity measure:

$$\psi_1 = \begin{cases} 1, & \Delta_{\vec{s}} \vec{v} < 0 \\ 0, & \Delta_{\vec{s}} \vec{v} \geq 0 \end{cases}, \qquad \psi_0 = \frac{|\nabla \cdot \vec{v}|}{\|\nabla \vec{v}\|}$$

$\vec{s}_1$ is the direction of maximal compression: $\min_{|\vec{s}|=1} \Delta_{\vec{s}} \vec{v} = \min_{|\vec{s}|=1} \vec{s} \cdot \varepsilon(\vec{v}) \cdot \vec{s} = \lambda_1 = \Delta_{\vec{s}_1} \vec{v}$.

# Stress: Directional Length Scale

**We define the length scale in direction $\vec{s}$ relative to an initial length scale field $\ell_0(\vec{x})$ on $\Omega(t_0)$.**

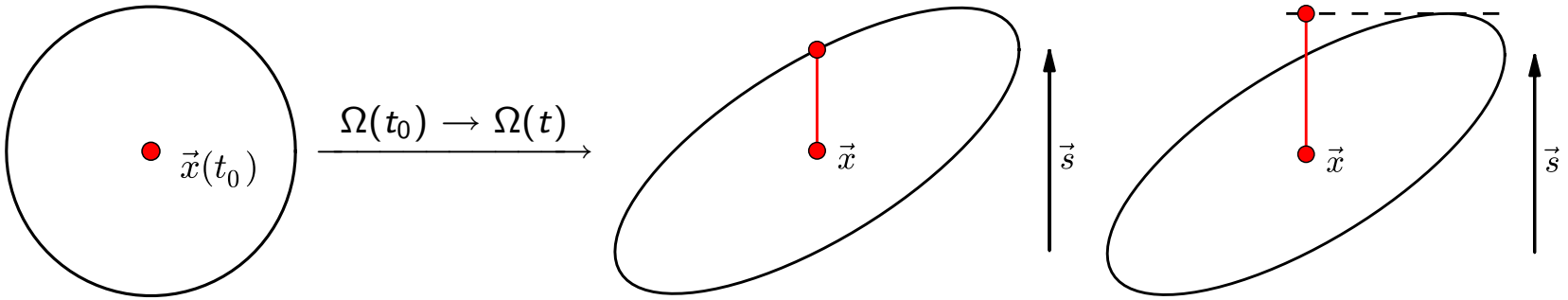


Using the Jacobian $J$ of the mapping $\hat{\Omega} \longrightarrow \Omega(t)$ the two versions can be written as:

$$\ell_{\vec{s}}(\vec{x}) = \ell_0 \frac{|\vec{s}|}{|J^{-1}\vec{s}|}$$

$$\ell_{\vec{s}}(\vec{x}) = \ell_0 \frac{|J^{\top}\vec{s}|}{|\vec{s}|}$$

We have the following options to define $\ell_0(\vec{x})$:

- global constant, e.g. in 2D $\ell_0 = (\text{tot. area}/\text{num. of zones})^{1/2}$ (meshes close to uniform)
- smoothed version of a local mesh size function (meshes with local refinement)
- smoothed or constant function based on $x$-direction mesh size (1D problems)

# Stress: Elastic-Plastic Deformation

To model elastic-plastic solids, we add a stress deviator tensor $s$ to the total stress tensor $\sigma$:

$$\sigma(\vec{x}) = -p(\vec{x})\mathbf{I} + \sigma_a(\vec{x}) + s(\vec{x}).$$

As with the other stress terms, the stress deviator tensor varies inside a zone.
We utilize an incremental stress/strain relation and compute the Jaumann objective stress rate at each quadrature point as

$$\frac{ds}{dt} = g(s, \vec{v}, \mu_s) \equiv 2\mu_s \left( \frac{1}{2}(\nabla\vec{v} + \vec{v}\nabla) - \frac{1}{3}\nabla\cdot\vec{v} \right) + \frac{s(\nabla\vec{v} - \vec{v}\nabla) - (\nabla\vec{v} - \vec{v}\nabla)s}{2}.$$

We use the Von Mises yield condition and a simple "radial-return" method for calculating transition to plastic flow:

$$f(s, Y) = \sqrt{\frac{2}{3}\frac{Y^2}{Tr(s^2)}}, \quad if: \ f > 1, \ then: \ f \mapsto 1; \quad s \mapsto fs.$$

Each component of the stress rate is discretized using a density weighted projection onto the discontinous internal energy basis, $\phi$.

$$\mathbf{M_e}\frac{\mathrm{d}\mathbf{s}}{\mathrm{d}t} = \mathbf{g} \equiv \int_\Omega (\rho g)\,\phi$$

Therefore, we only store the stress rate at the energy degrees of freedom instead of each quadrature point.

**$Q_1$ stress rate degrees of freedom on the reference element**

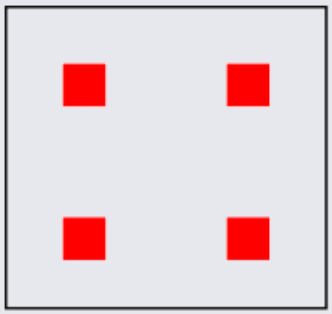

# Generalized Corner Forces

The computational kernel of our method is the evaluation of the **Generalized Corner Force** matrix

$$\mathbf{F}_{ij} = \int_{\Omega(t)} (\sigma : \nabla \vec{w}_i)\, \phi_j$$

**Semi-discrete finite element method**

**Momentum Conservation:** $\mathbf{M_v} \dfrac{\mathrm{d}\mathbf{v}}{\mathrm{d}t} = -\mathbf{F} \cdot \mathbf{1}$

**Energy Conservation:** $\mathbf{M_e} \dfrac{\mathrm{d}\mathbf{e}}{\mathrm{d}t} = \mathbf{F}^T \cdot \mathbf{v}$

**Equation of Motion:** $\dfrac{\mathrm{d}\mathbf{x}}{\mathrm{d}t} = \mathbf{v}$

**Stress Deviator Rate:** $\mathbf{M_e} \dfrac{\mathrm{d}\mathbf{s}}{\mathrm{d}t} = \mathbf{g}$

- $\mathbf{F}$ can be assembled locally from zonal corner force matrices $\mathbf{F}_z$.
- Generalized SGH "corner forces": $\mathbf{F}_z$ is 8x1 for $Q_1$-$Q_0$, 18x4 for $Q_2$-$Q_1$, 32x9 for $Q_3$-$Q_2$ (2D).
- Locally FLOP-intensive evaluation of $\mathbf{F}_z$ requires high order quadrature $\{(\alpha_k, \hat{\vec{q}}_k)\}$

$$(\mathbf{F}_z)_{ij} = \int_{\Omega_z(t)} (\sigma : \nabla \vec{w}_i)\, \phi_j \approx \sum_k \alpha_k \hat{\sigma}(\hat{\vec{q}}_k) : \mathbf{J}_z^{-1}(\hat{\vec{q}}_k) \hat{\nabla} \hat{\vec{w}}_i(\hat{\vec{q}}_k)\, \hat{\phi}_j(\hat{\vec{q}}_k) |\mathbf{J}_z(\hat{\vec{q}}_k)|$$

- Pressure is a function computed through the EOS in $\{\hat{\vec{q}}_k\}$ ("sub-zonal pressure").

# Generalized Corner Forces

The computational kernel of our method is the evaluation of the **Generalized Corner Force** matrix

$$\mathbf{F}_{ij} = \int_{\Omega(t)} (\sigma : \nabla \vec{w}_i)\, \phi_j$$

**Semi-discrete finite element method**

**Momentum Conservation:** $\mathbf{M_v} \dfrac{\mathrm{d}\mathbf{v}}{\mathrm{d}t} = -\mathbf{F} \cdot \mathbf{1}$

**Energy Conservation:** $\mathbf{M_e} \dfrac{\mathrm{d}\mathbf{e}}{\mathrm{d}t} = \mathbf{F}^T \cdot \mathbf{v}$

**Equation of Motion:** $\dfrac{\mathrm{d}\mathbf{x}}{\mathrm{d}t} = \mathbf{v}$

**Stress Deviator Rate:** $\mathbf{M_e} \dfrac{\mathrm{d}\mathbf{s}}{\mathrm{d}t} = \mathbf{g}$

By strong mass conservation, the above algorithm gives **exact semi-discrete energy conservation for any choice of velocity and energy spaces** (including continuous energy).

$$\frac{\mathrm{d}E}{\mathrm{d}t} = \frac{\mathrm{d}}{\mathrm{d}t}\left(\int_{\Omega(t)} \rho \frac{|\vec{v}|^2}{2} + \rho e\right) = \frac{\mathrm{d}}{\mathrm{d}t}\left(\frac{\mathbf{v}\cdot\mathbf{M_v}\cdot\mathbf{v}}{2} + \mathbf{1}\cdot\mathbf{M_e}\cdot\mathbf{e}\right)$$

$$= \mathbf{v}\cdot\mathbf{M_v}\cdot\frac{\mathrm{d}\mathbf{v}}{\mathrm{d}t} + \mathbf{1}\cdot\mathbf{M_e}\cdot\frac{\mathrm{d}\mathbf{e}}{\mathrm{d}t} = -\mathbf{v}\cdot\mathbf{F}\cdot\mathbf{1} + \mathbf{1}\cdot\mathbf{F}^T\cdot\mathbf{v} = 0.$$

Any "compatible hydro" method can be put into this framework for appropriate $\mathbf{M_v}$, $\mathbf{M_e}$ and $\mathbf{F}$.

# Time Integration

Let $Y = (\mathbf{v}; \mathbf{e}; \mathbf{x}; \mathbf{s})$. Then the semi-discrete equations can be written in the form:

$$\frac{\mathrm{d}Y}{\mathrm{d}t} = \mathcal{F}(Y, t)$$

where

$$\mathcal{F}(Y, t) = \begin{pmatrix} \mathcal{F}_v(\mathbf{v}, \mathbf{e}, \mathbf{x}, \mathbf{s}) \\ \mathcal{F}_e(\mathbf{v}, \mathbf{e}, \mathbf{x}, \mathbf{s}) \\ \mathcal{F}_x(\mathbf{v}, \mathbf{e}, \mathbf{x}, \mathbf{s}) \\ \mathcal{F}_s(\mathbf{v}, \mathbf{e}, \mathbf{x}, \mathbf{s}) \end{pmatrix} = \begin{pmatrix} -\mathbf{M_v}^{-1}\mathbf{F} \cdot \mathbf{1} \\ \mathbf{M_e}^{-1}\mathbf{F}^\top \cdot \mathbf{v} \\ \mathbf{v} \\ \mathbf{M_e}^{-1}\mathbf{g} \end{pmatrix}$$

Standard high order time integration techniques (e.g. explicit Runge-Kutta methods) can be applied to this system of nonlinear ODEs.

The standard methods may need modifications to ensure:

- Numerical stability of the scheme.
- Exact energy conservation.

Two of the options we use are:

- **RK2Avg** – midpoint RK2 method, modified for exact energy conservation.
- **RK4** – standard fourth order Runge-Kutta method.

# The RK2Avg Scheme

The midpoint Runge-Kutta second order scheme (**RK2**) reads

$$Y^{n+\frac{1}{2}} = Y^n + \frac{\Delta t}{2}\,\mathcal{F}(Y^n, t^n)$$
$$Y^{n+1} = Y^n + \Delta t\,\mathcal{F}(Y^{n+\frac{1}{2}}, t^{n+\frac{1}{2}})$$

We modify it for stability and energy conservation as follows (**RK2Avg**):

$$\mathbf{v}^{n+\frac{1}{2}} = \mathbf{v}^n - (\Delta t/2)\,\mathbf{M_v}^{-1}\mathbf{F}^n \cdot \mathbf{1}$$
$$\mathbf{e}^{n+\frac{1}{2}} = \mathbf{e}^n + (\Delta t/2)\,\mathbf{M_e}^{-1}(\mathbf{F}^n)^\top \cdot \mathbf{v}^{n+\frac{1}{2}}$$
$$\mathbf{x}^{n+\frac{1}{2}} = \mathbf{x}^n + (\Delta t/2)\,\mathbf{v}^{n+\frac{1}{2}}$$
$$\mathbf{s}^{n+\frac{1}{2}} = \mathbf{s}^n + (\Delta t/2)\,\mathbf{M_e}^{-1}\mathbf{g}^n$$

$$\mathbf{v}^{n+1} = \mathbf{v}^n - \Delta t\,\mathbf{M_v}^{-1}\mathbf{F}^{n+\frac{1}{2}} \cdot \mathbf{1}$$
$$\mathbf{e}^{n+1} = \mathbf{e}^n + \Delta t\,\mathbf{M_e}^{-1}(\mathbf{F}^{n+\frac{1}{2}})^\top \cdot \bar{\mathbf{v}}^{n+\frac{1}{2}}$$
$$\mathbf{x}^{n+1} = \mathbf{x}^n + \Delta t\,\bar{\mathbf{v}}^{n+\frac{1}{2}}$$
$$\mathbf{s}^{n+1} = \mathbf{s}^n + \Delta t\,\mathbf{M_e}^{-1}\mathbf{g}^{n+\frac{1}{2}}$$

Here $\mathbf{F}^n = \mathbf{F}(Y^n)$ and $\bar{\mathbf{v}}^{n+\frac{1}{2}} = (\mathbf{v}^n + \mathbf{v}^{n+1})/2$. The change in kinetic (KE) and internal (IE) energy is

$$KE^{n+1} - KE^n = (\mathbf{v}^{n+1} - \mathbf{v}^n) \cdot \mathbf{M_v} \cdot \bar{\mathbf{v}}^{n+\frac{1}{2}} = -\Delta t\,(\mathbf{F}^{n+\frac{1}{2}} \cdot \mathbf{1}) \cdot \bar{\mathbf{v}}^{n+\frac{1}{2}}$$
$$IE^{n+1} - IE^n = \mathbf{1} \cdot \mathbf{M_e} \cdot (\mathbf{e}^{n+1} - \mathbf{e}^n) = \Delta t\,\mathbf{1} \cdot (\mathbf{F}^{n+\frac{1}{2}})^\top \cdot \bar{\mathbf{v}}^{n+\frac{1}{2}}).$$

**Therefore the discrete total energy is preserved**: $KE^{n+1} + IE^{n+1} = KE^n + IE^n$.

# Example: 1D Elastic Wave with Non-Linear EOS

We consider a polynomial EOS of the form:

$$p(\mu, e) = \mu + \mu^2 + \mu^3 + (1 + \mu + \mu^2)\frac{e}{\rho_0}; \quad \mu \equiv (\frac{\rho}{\rho_0} - 1)$$

- Simple 1D elastic wave propgation with constant shear modulus
- Test self convergence using time refinement
- No artificial viscosity is used
- Wall boundary conditions
- Velocity is initialized with a sinusoidal profile:

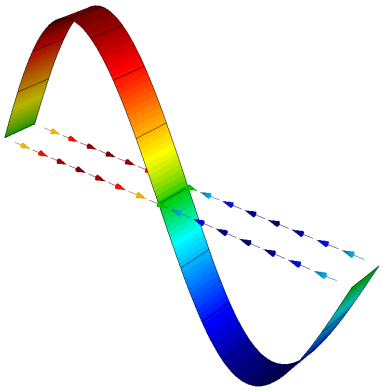

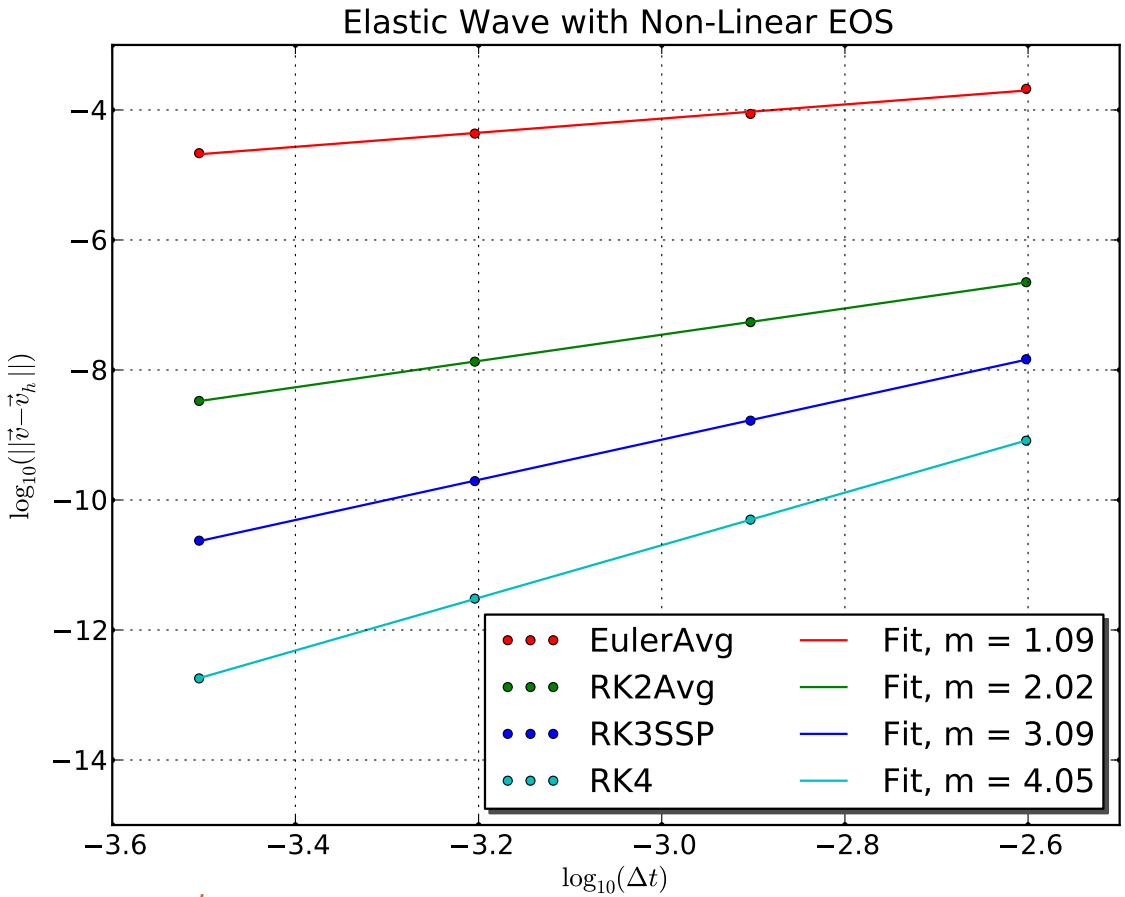


Up to $4^{th}$ order convergence in time for smooth elastic problem with non-linear EOS.

# Example: 2D Taylor-Green Vortex

- 2D Taylor–Green vortex problem run to $t = 0.75$
- Manufactured solution, no artificial viscosity is used

Q2-Q1-RK2Avg

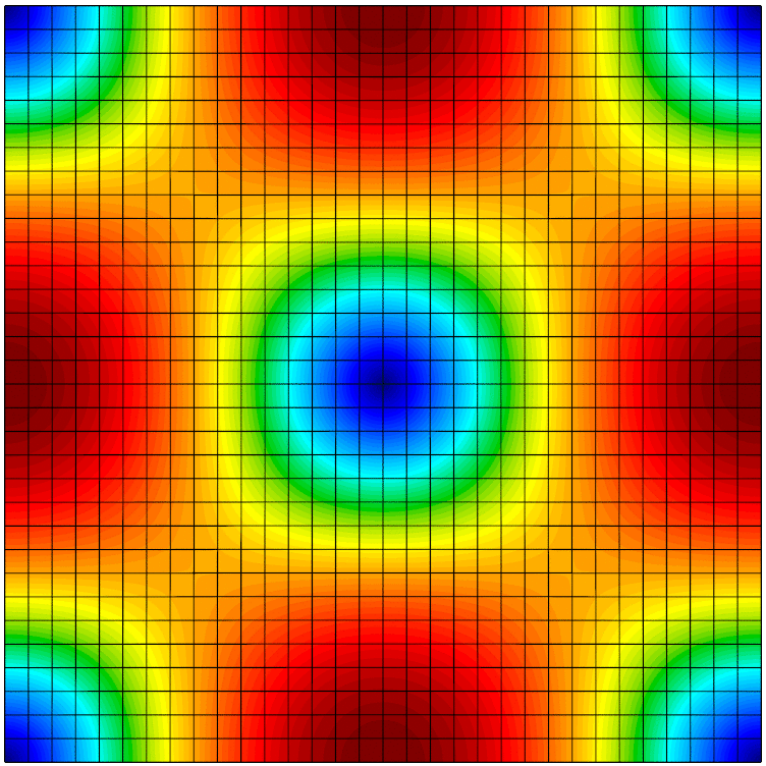

32x32 structured grid

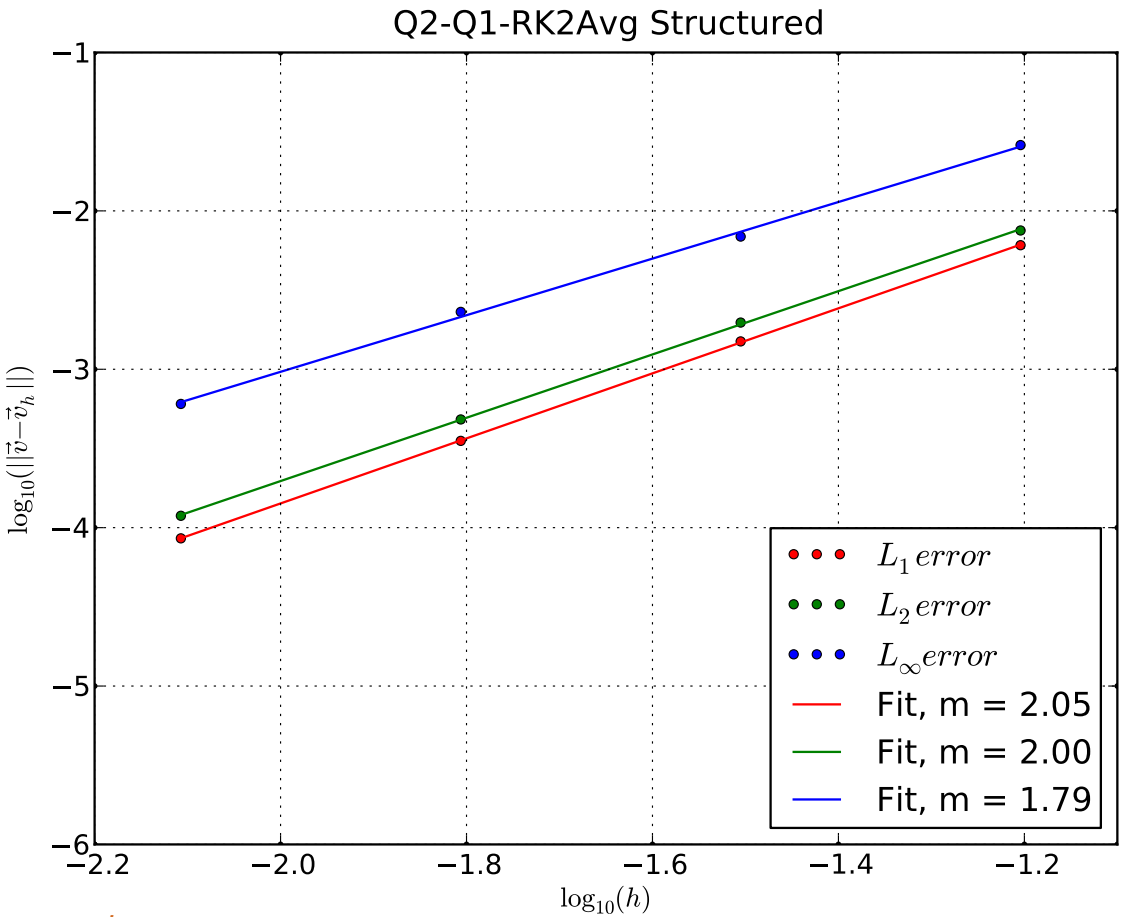


$2^{nd}$ order convergence in space and time for smooth problem.

# Example: 2D Taylor-Green Vortex

- 2D Taylor–Green vortex problem run to $t = 0.75$
- Manufactured solution, no artificial viscosity is used

Q3-Q2-RK4

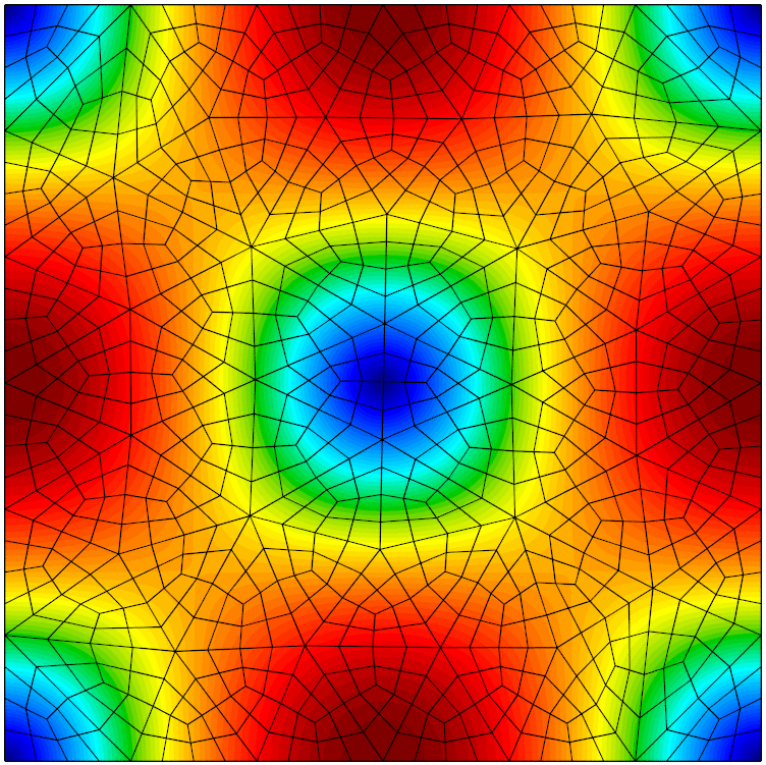

Unstructured grid

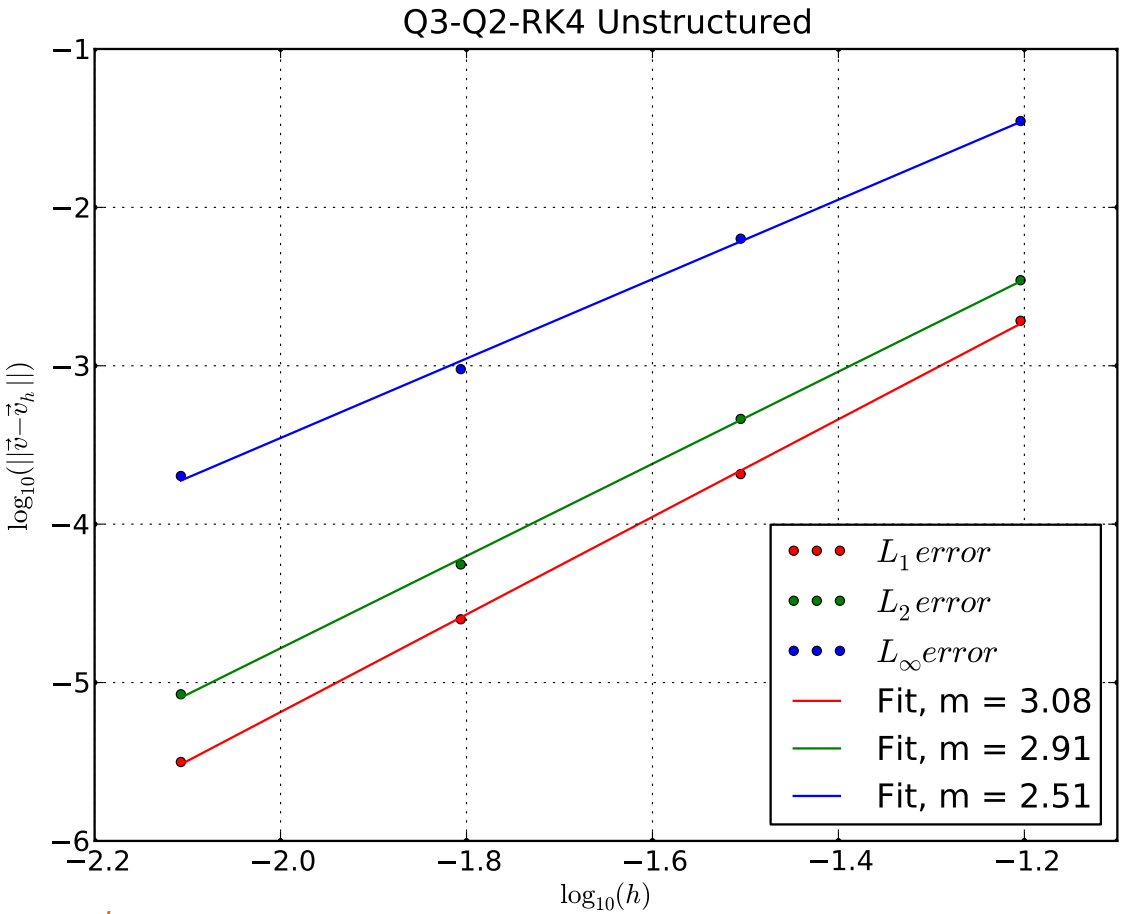


$3^{rd}$ order convergence in space and time for smooth problem.

# Example: 1D Elastic-Plastic Shock Wave

1D elastic-plastic shock wave test problem and analytic solution developed by G. Bazan at LLNL.

- Problem consists of a solid flyer impacting a stationary solid target
- Two shock state with an "elastic precursor" followed by a second plastic shock
- Verifies ability of a method to propagate an elastic-plastic shock

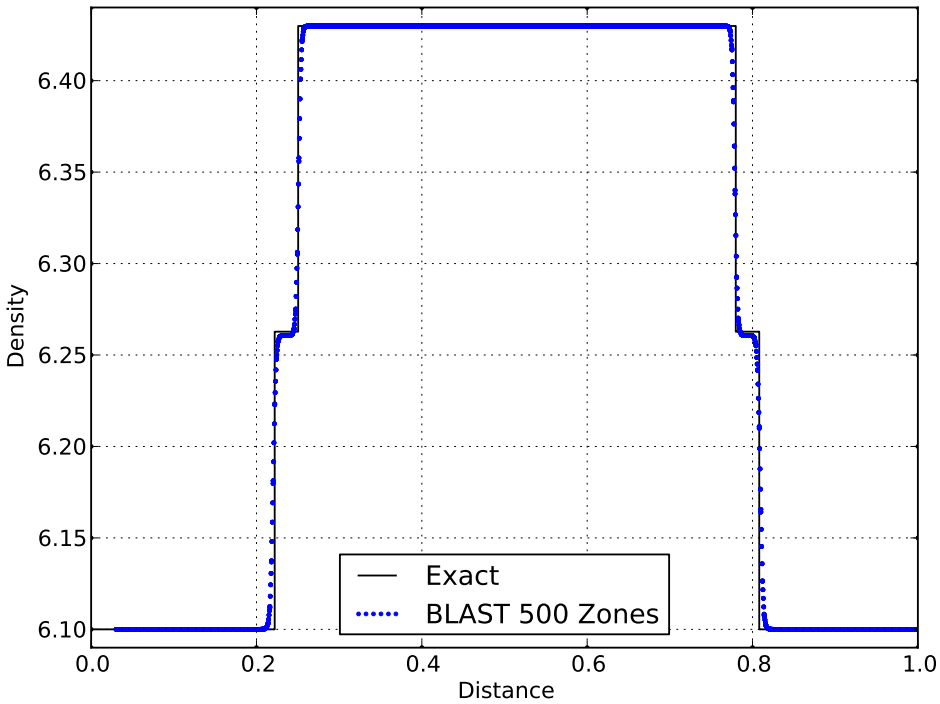


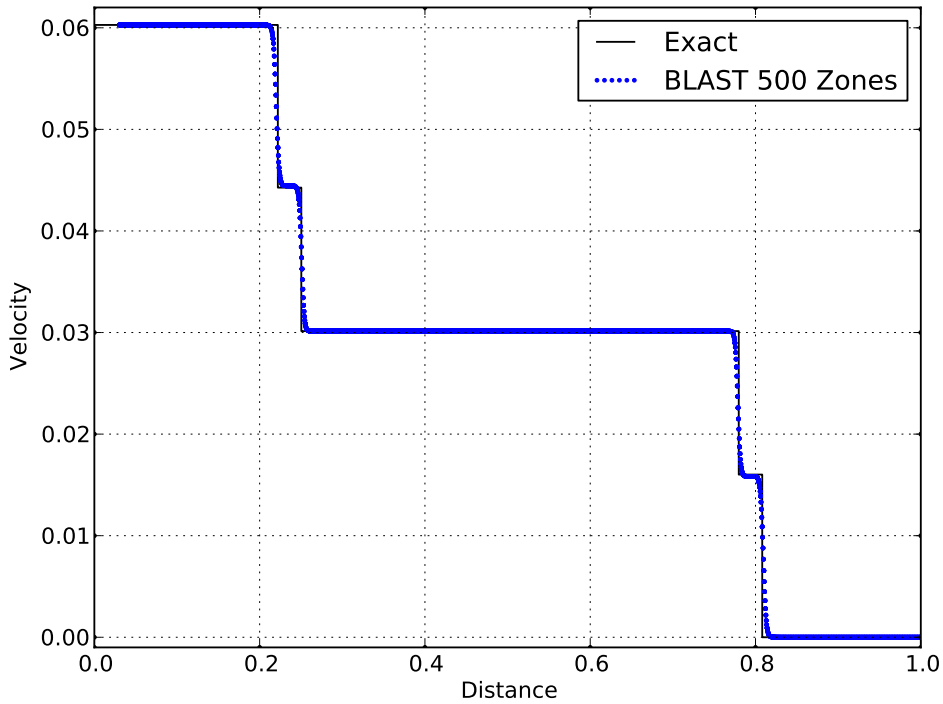

# Example: 2D Sedov Blast Wave on Cartesian Grid

Density and Curvilinear Mesh, 20x20 zones

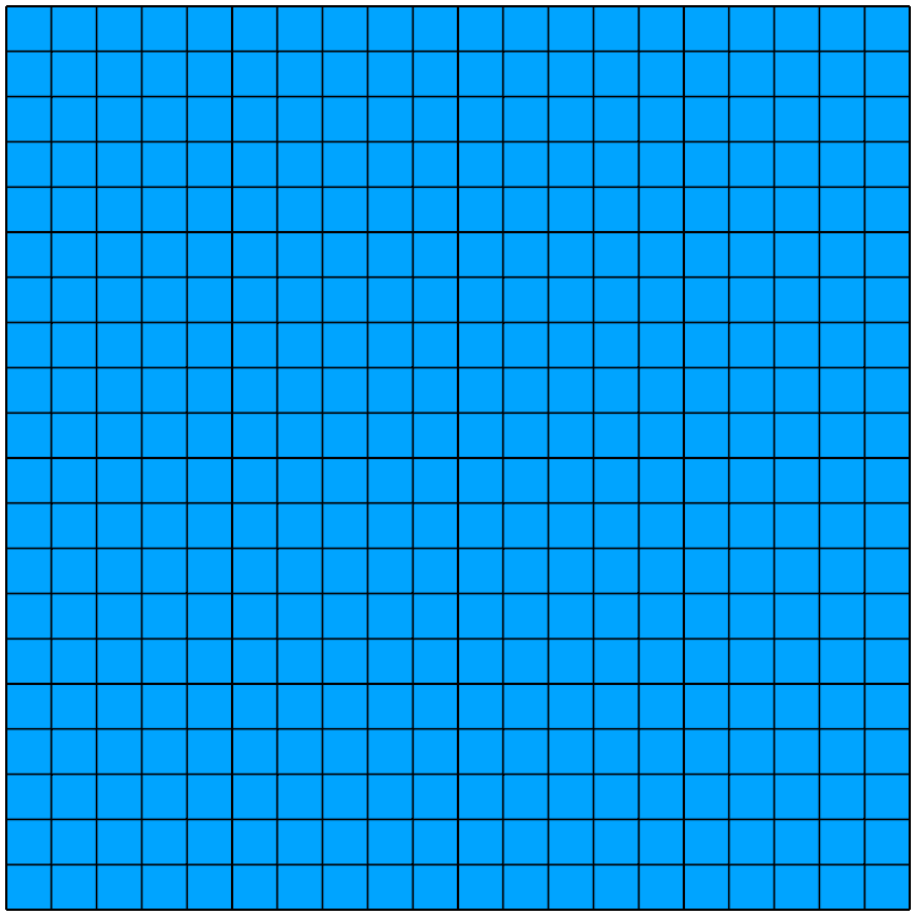

- Symmetry is preserved

Exact Deformation

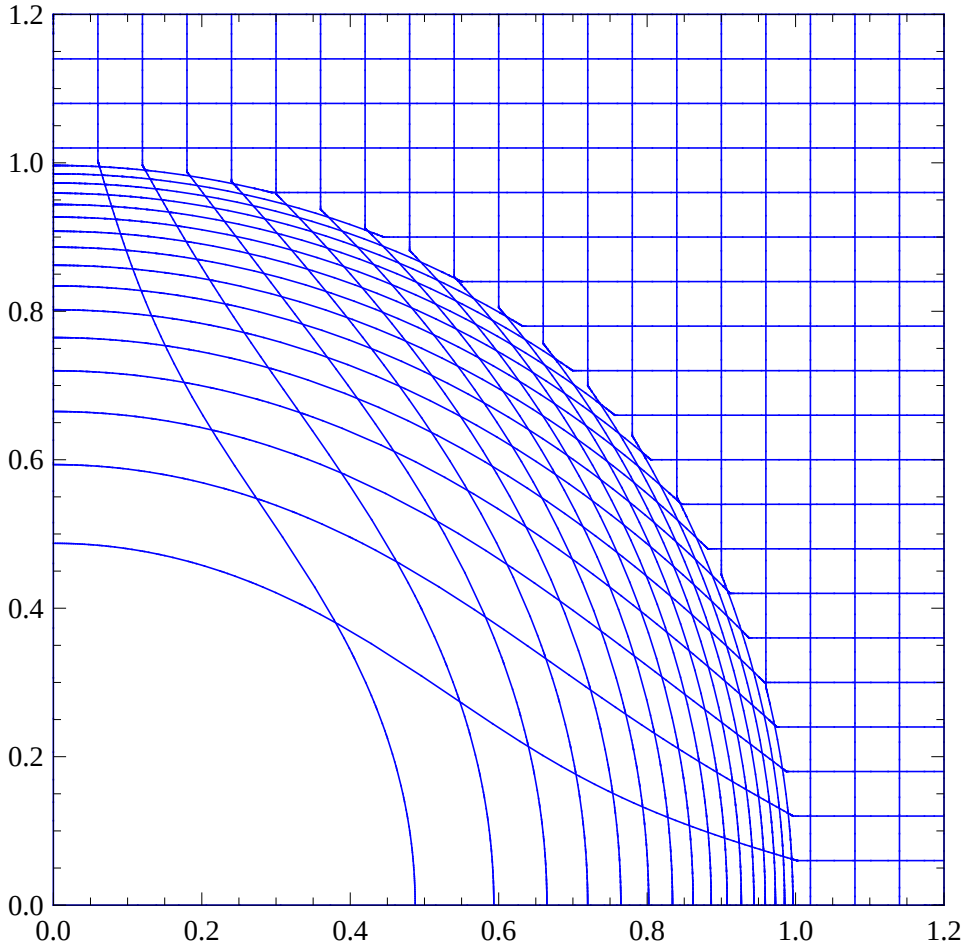


- Curved mesh gives better approximation

# Example: 2D Sedov Blast Wave on Cartesian Grid

Density Scatter Plots

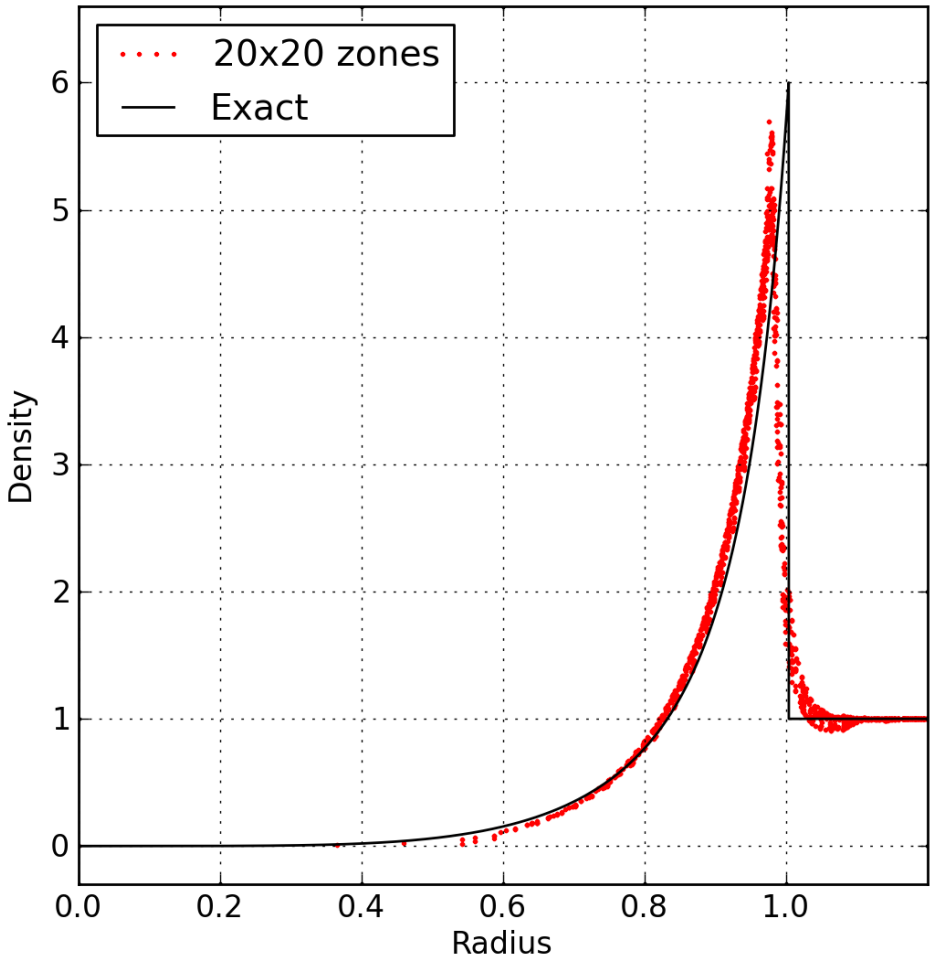


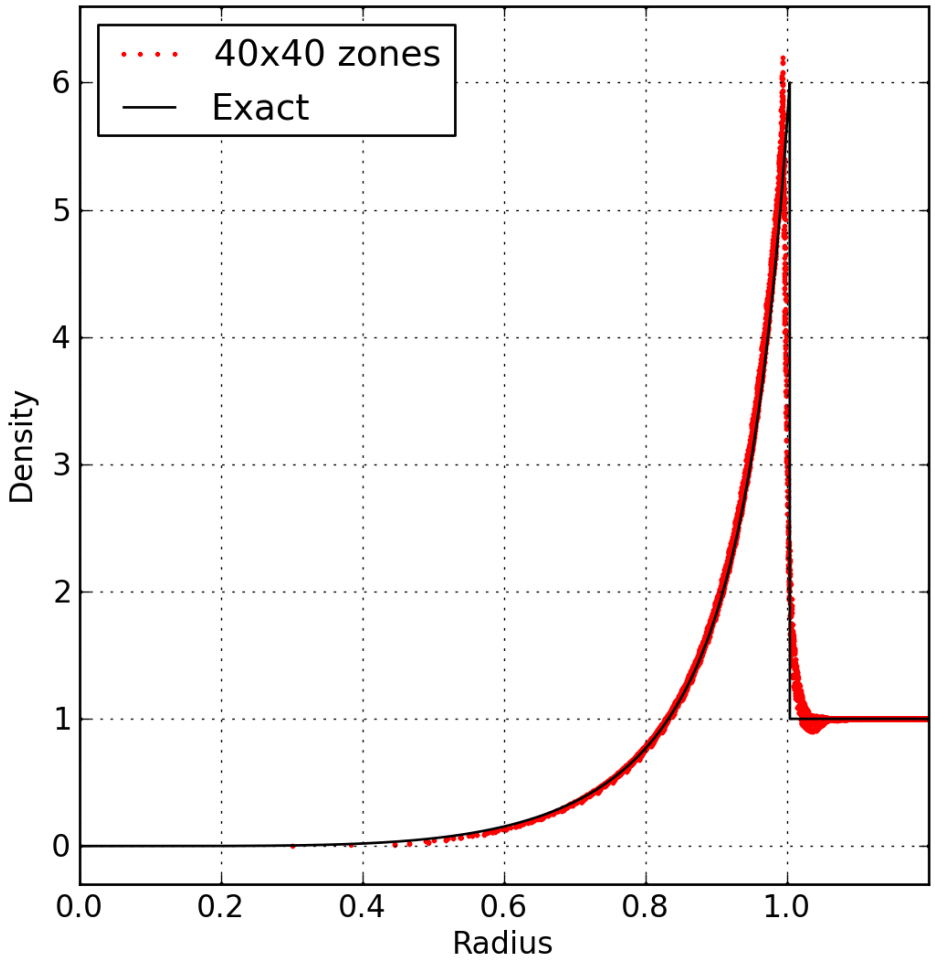


- Evaluated at 9 points/zone
- Converges to exact solution

# Example: 2D Sedov Blast Wave on Cartesian Grid

Density Scatter Plots

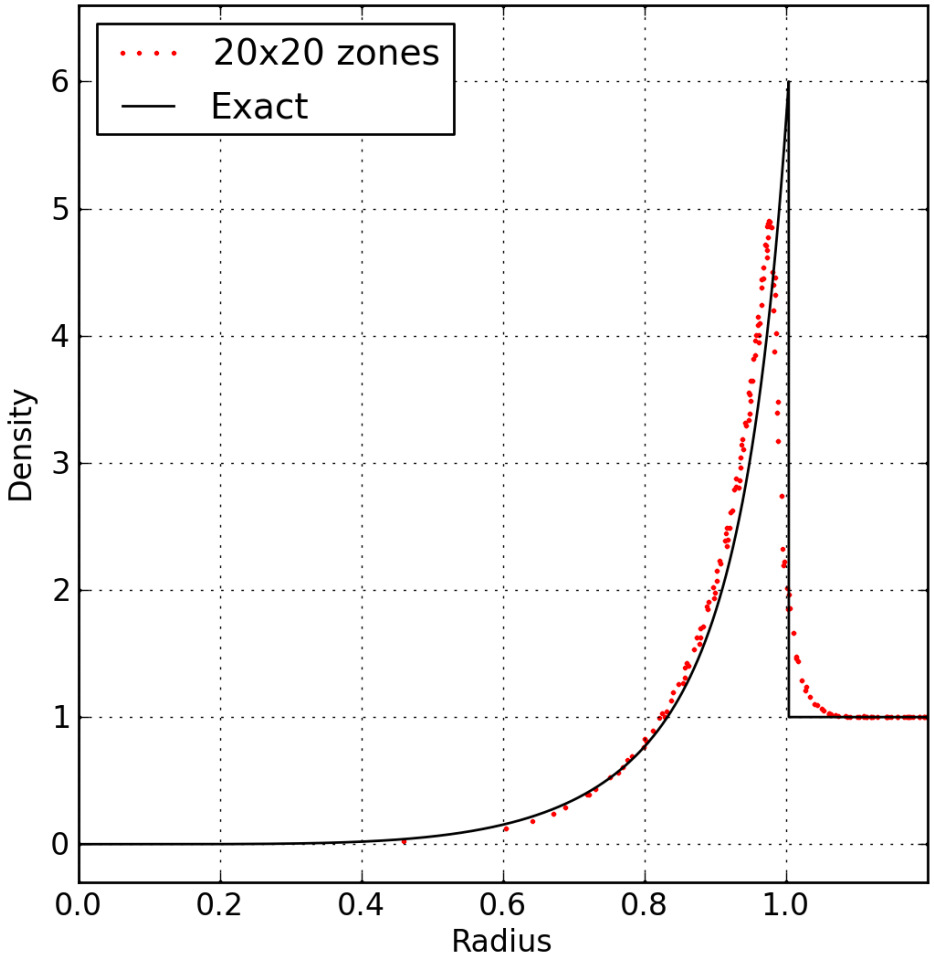


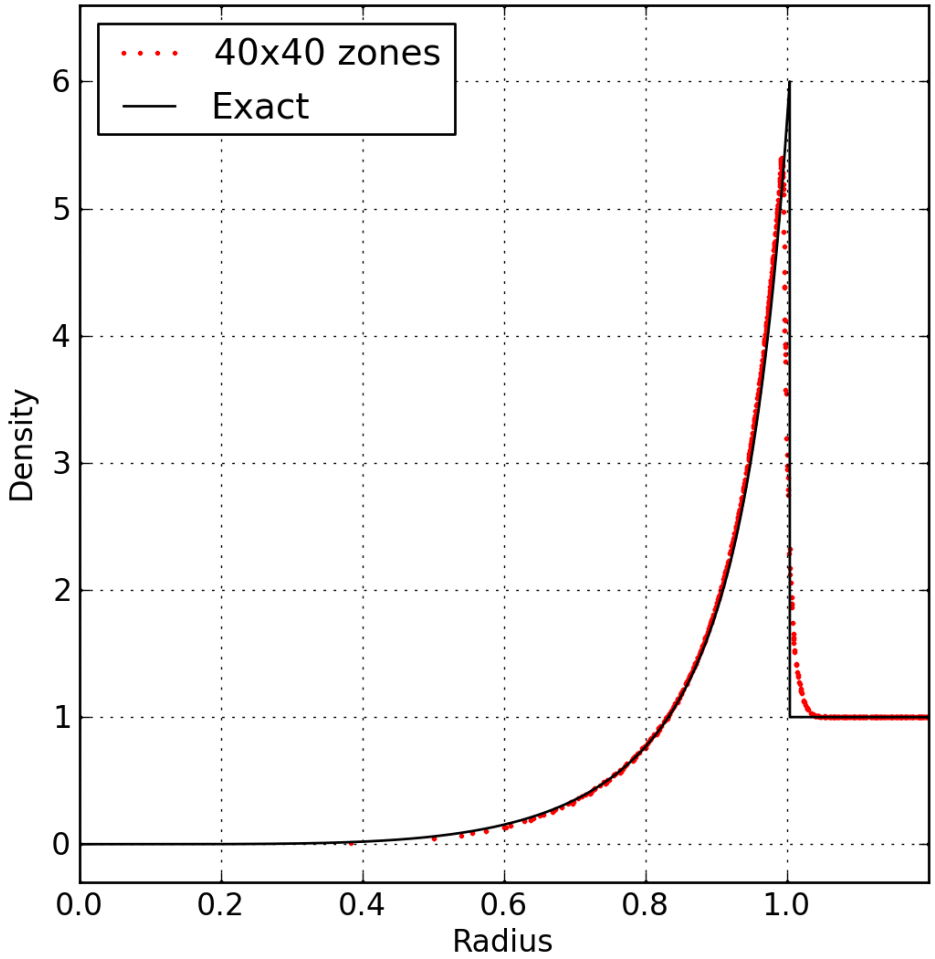


- Evaluated at zone centers
- No undershoots and overshoots

# Example: Saltzman Piston

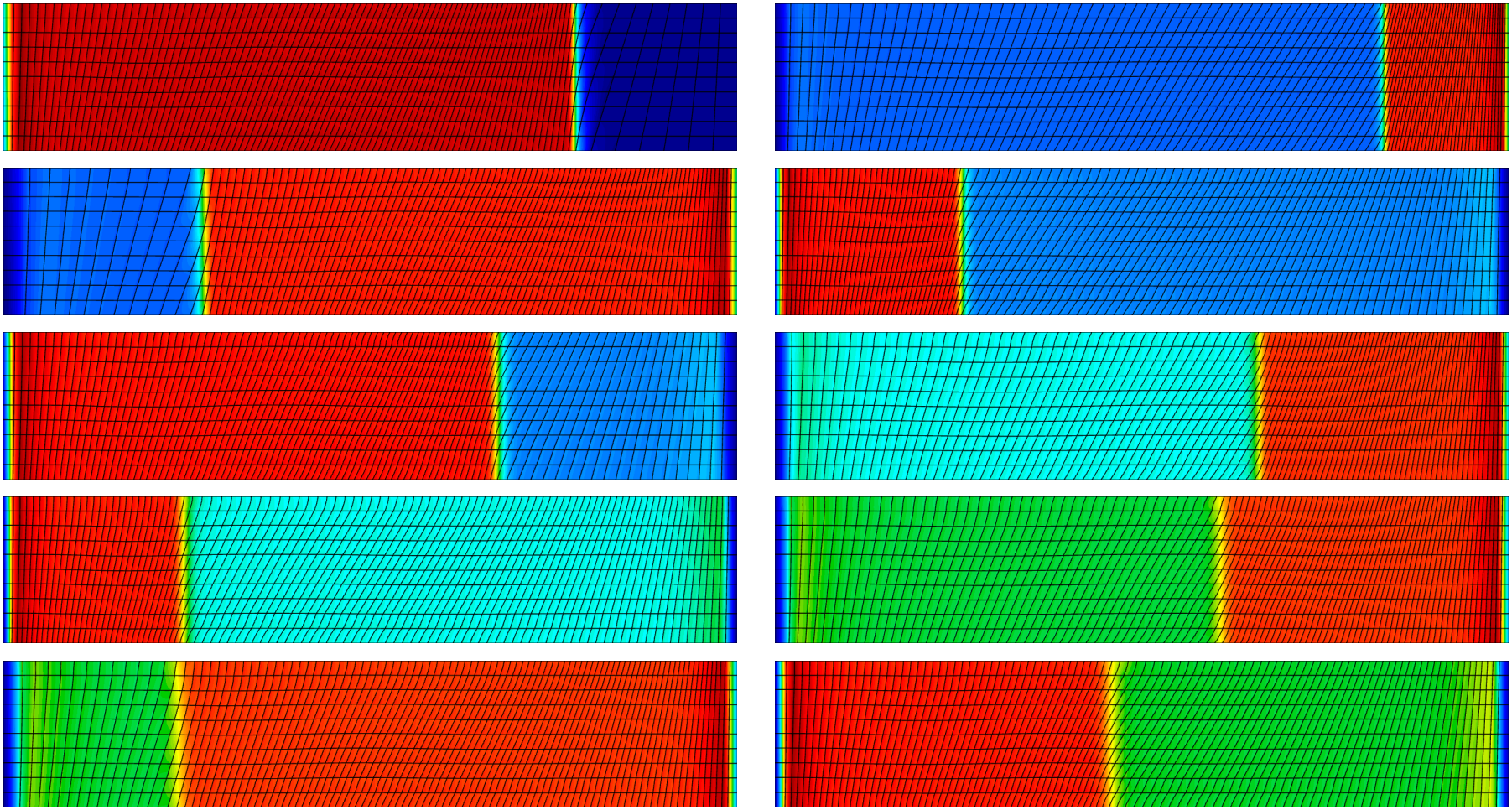

Density and mesh for Saltzman piston problem at $t = 0.7$, 0.8, 0.88, 0.92, 0.94, 0.96, 0.975, 0.985, 0.987 and 0.99 for a total of 6 bounces. (We can run this further.)

Each image is rescaled to an aspect ratio of 5 : 1.

# Example: 2D Single Material Rayleigh-Taylor Instability

Suggested by A. Barlow / D. Youngs, the material interface is flat. Initial velocity is divergence free with a slip line at the interface, initial pressure is from hydrostatic equilibrium:

AMR-ALE with 4 Refinement Levels

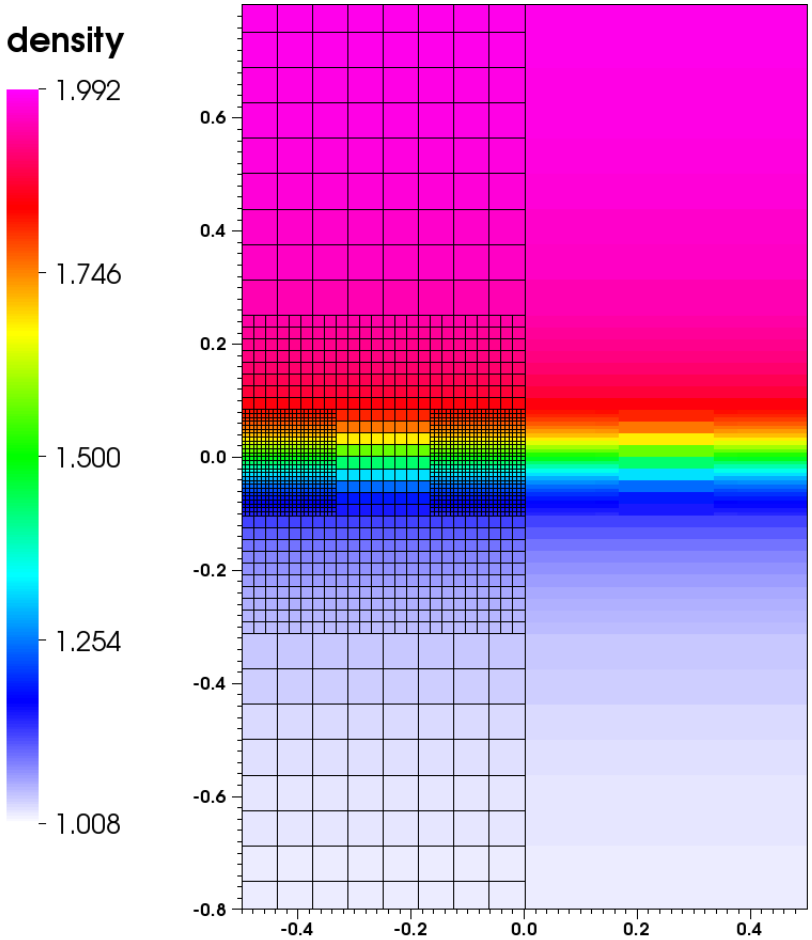


BLAST Q3Q2

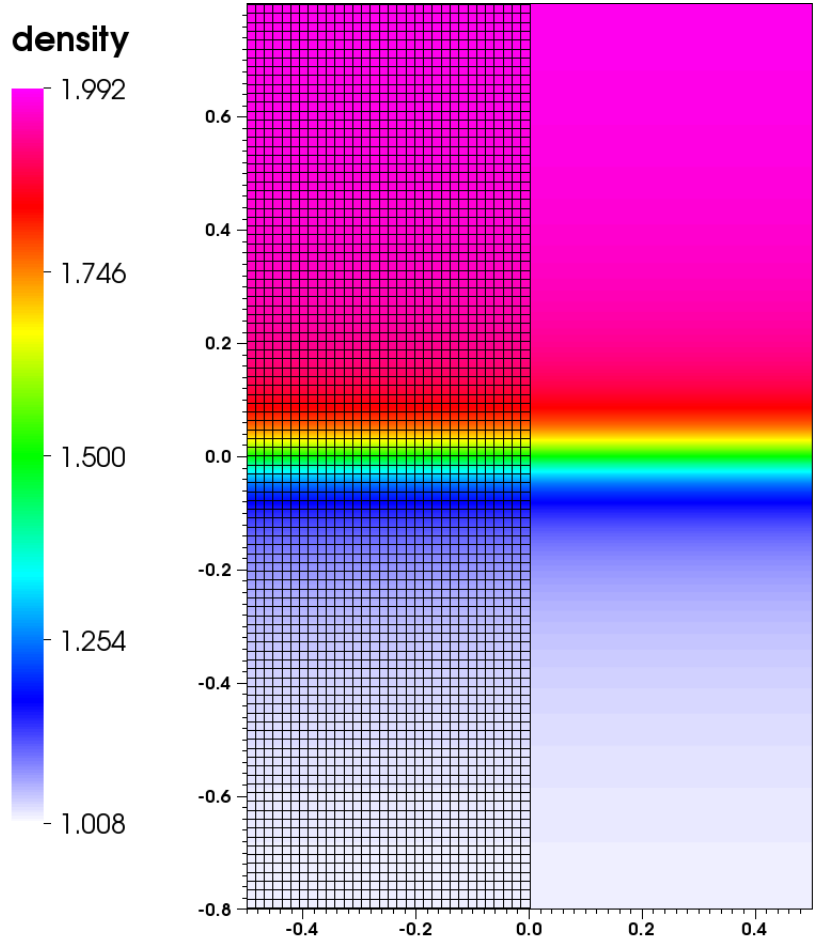


The high order Lagrangian calculation is in good agreement with the AMR-ALE result.

# Example: 2D Single Material Rayleigh-Taylor Instability

- Compressible fluids
- Single material with a smooth density gradient
- Heavy fluid on top of a light fluid
- Initially perturbed interface
- Constant initial pressure
- Small downward acceleration

High order methods allow the problem to run longer in time and resolve more of the flow features.

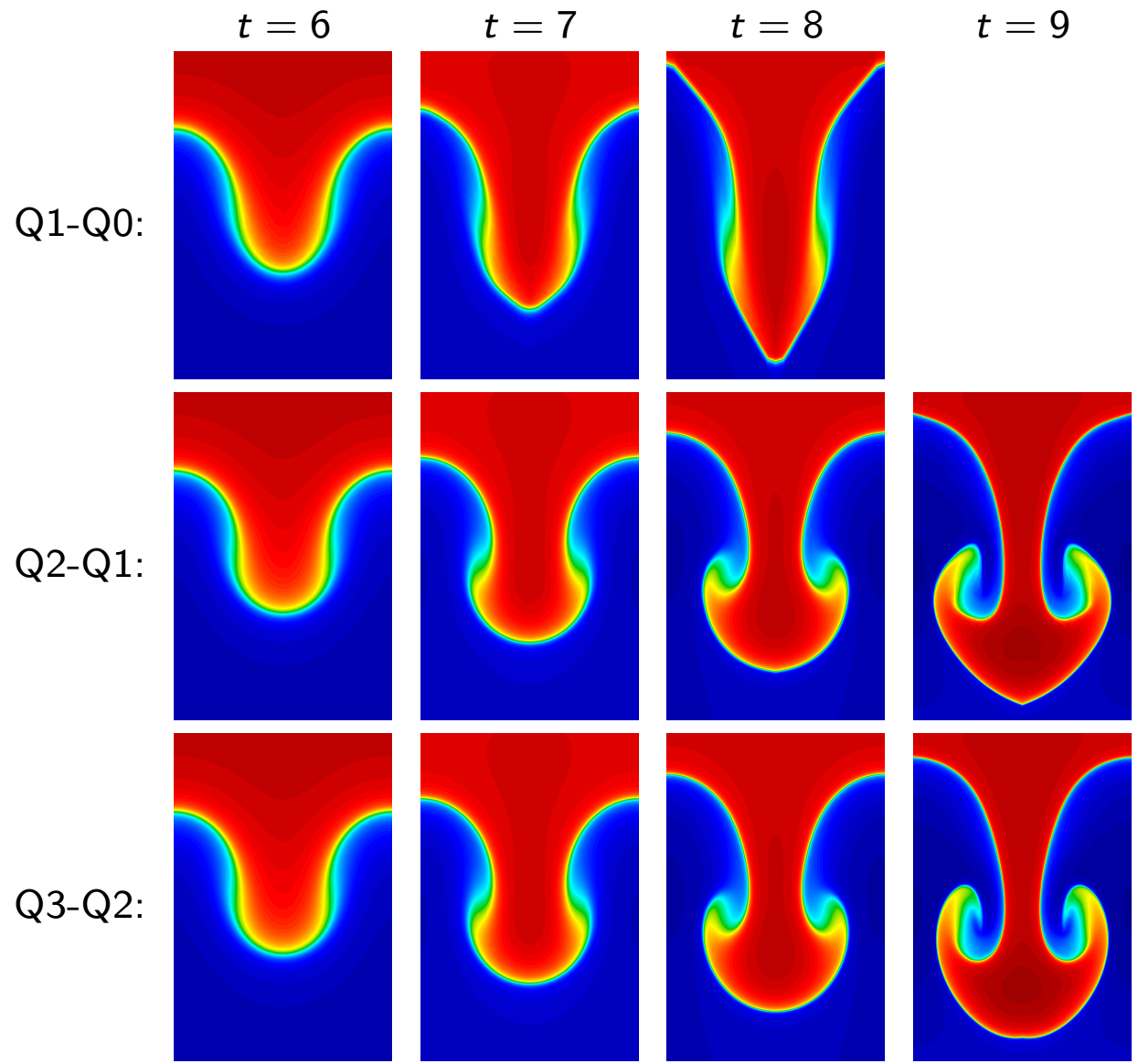

# Conclusions

We have developed a **general energy-conserving, high-order finite element discretization of the Euler equations in a Lagrangian frame**.

**Benefits of our high-order discretization framework:**

- More accurate capturing of the geometrical features of a flow region using curvilinear zones.
- Higher order spatial accuracy.
- Support for general high order temporal discretizations for systems of ODEs.
- Exact total energy conservation by construction.
- Generality with respect to choice of kinematic and thermodynamic spaces.
- No need for ad-hoc hourglass filters.
- Sharper resolution of the shock front. Shocks can be represented within a single zone.
- Substantial reduction in mesh imprinting.

**We have shown just a small set of example results; see Part II for many more numerical results.**

**Publications:**

V. Dobrev, T. Ellis, Tz. Kolev and R. Rieben, *"Curvilinear Finite Elements for Lagrangian Hydrodynamics"*, International Journal for Numerical Methods in Fluids, 65 (11-12), pp. 1295–1310, 2011.

Tz. Kolev and R. Rieben, *"A Tensor Artificial Viscosity Using a Finite Element Approach"*, Journal of Computational Physics, 228(22), pp. 8336–8366, 2009.